Shape of the 4.438 MeV γ-ray line of ^{12}C from proton and α-particle induced reactions on ^{12}C and ^{16}O

J. Kiener, N. de Séréville, and V. Tatischeff

CSNSM, IN2P3-CNRS et Université Paris-Sud, Bâtiments 104 et 108, F-91405 Campus Orsay, France

We calculated in detail the angular distribution of γ rays and the resulting shape of the γ-ray line produced by the nuclear deexcitation of the 4.439 MeV state of ^{12}C following proton and α-particle interactions with ^{12}C and ^{16}O in the energy range from threshold to 100 MeV per nucleon, making use of available experimental data. In the proton energy range from 8.6 to 20 MeV, the extensive data set of a recent accelerator experiment on γ-ray line shapes and angular distributions was used to deduce parametrizations for the γ-ray emission of the 2^+, 4.439 MeV state of ^{12}C following inelastic proton scattering off ^{12}C and proton induced spallation of ^{16}O. At higher proton energies and for α-particle induced reactions, optical model calculations were the main source to obtain the needed reaction parameters for the calculation of γ-ray line shapes and angular distributions. Line shapes are predicted for various interaction scenarios of accelerated protons and α particles in solar flares.

I. INTRODUCTION

The γ-ray line at 4.438 MeV from the deexcitation of the first excited state of ^{12}C is one of the strongest nuclear lines, clearly visible in several energetic solar flares, which were observed in particular by the Gamma Ray Spectrometer aboard the SMM satellite [1] and one of the best candidates for an observation at γ-ray energies of the interaction of low energy cosmic rays in nearby molecular clouds [2]. It is mainly produced by inelastic scattering of energetic protons and α-particles off ^{12}C and by the spallation of ^{16}O by the same particles [3]. This line is also produced in reverse kinematics by accelerated ^{12}C and ^{16}O bombarding the ambient hydrogen and helium nuclei, with however a large Doppler broadening due to the high velocities of the emitting ^{12}C nucleus, which makes its detection much more difficult. In the following we will refer to γ-ray lines produced by light ion bombardment of the ambient gas as the narrow component and to γ rays produced by accelerated heavy ions as the broad component.

Accordingly, the intensity and shape of the narrow component of the 4.438 MeV line depend on the properties of the accelerated light particle spectrum and the ^{12}C and ^{16}O abundances in the interaction site. The narrow line intensities from various isotopes can be used to derive accelerated particle and ambient gas abundances, as it has been done for example by Murphy *et al.* [4] for the solar flare of 1981 April 27. More detailed information on the energy spectrum of the accelerated particles and their directional distribution at the interaction site may, however, only be obtained by a detailed line shape analysis.

Murphy, Kozlovsky, and Ramaty [5] investigated the impact of different accelerated particle angular distributions on the narrow component of the 4.438 MeV γ-ray line produced by the $p + {}^{12}$C reaction. The shape of the broad component has been discussed by Bykov, Bozhokin, and Bloemen [6] and by Kozlovsky, Ramaty, and Lingenfelter [7]. These studies are based on the experimentally well-known excitation

functions, some available experimental data on differential cross sections, few published results on measured line shapes, and theoretical arguments. For the spallation reaction, the situation is similar with respect to available experimental data. The excitation function is experimentally determined from threshold up to over 100 MeV, but few data are available on differential cross sections and line shapes.

In order to put the calculations for the 4.438 MeV line on a firmer basis, we use additionally to the already published data the extensive data set on γ-ray angular distributions and γ-ray line shapes for the ^{12}C$(p,p\gamma)$ and ^{16}O$(p,p\alpha\gamma)$ reaction, obtained in a recent accelerator experiment at Orsay [8]. For the spallation reaction, the reproduction of the observed line shapes for proton energies between 16 and 20 MeV proved to be only sensitive to the mean excitation energy of the α-particle emitting intermediate states of ^{16}O. Estimations of the mean excitation energy for higher proton energies and for the differential cross sections are based on published data in the proton energy range 40–50 MeV and optical model (OM) calculations.

For proton inelastic scattering, we adopted a method similar to that of Murphy, Kozlovsky, and Ramaty [5] for line shape calculations. Two independent amplitudes for the magnetic substate population of the 2^+ level and a phase shift were adjusted to reproduce both the experimental line shapes and the laboratory γ-ray angular distributions in the proton energy range from 8.6 to 19.75 MeV. The extrapolations to higher energies are based on OM calculations using phenomenological potential parameters, which proved to give an excellent reproduction of measured differential cross sections for nucleon elastic and inelastic scattering off ^{12}C at projectile energies $E \approx 20$–100 MeV [9].

α-particle inelastic scattering off ^{12}C and spallation of ^{16}O suffer from a complete absence of published data on line shapes. Therefore, estimations of the mean excitation energy in ^{16}O for the spallation reaction were entirely based on OM calculations and an experimental α-particle spectrum at $E_\alpha = 60$ MeV. For the inelastic scattering reaction, differential

cross sections $d\sigma/d\Omega_\alpha$ and some laboratory γ-ray angular distributions have been used to find the parameters for the γ-ray emission based on the population amplitude method at α-particle energies below 20 MeV, while at higher energies the needed parameters were obtained from OM calculations.

In the last section we discuss the production of the 4.438 MeV line in solar flares and show some calculated shapes for the narrow component of the 4.438 MeV line induced by proton and α-particle interactions in the solar atmosphere as it may be observed by the HESSI spacecraft [10].

II. THE SPALLATION REACTION ^{16}O$(p,x\gamma)^{12}$C

Total cross section data are reported by Dyer *et al.* [11] for $E_p = 14$–23 MeV, Lesko *et al.* [12] for $E_p = 20, 30, 33, 40,$ and 50 MeV, Lang *et al.* [13] at $E_p = 40$ MeV, Zobel *et al.* [14] at $E_p = 12.1, 28.2, 48.3,$ and 145 MeV, and by Foley *et al.* [15] at $E_p = 146$ MeV. From threshold to 23 MeV, we used the data of Ref. [11], which are in agreement with those of Refs. [12,14]. There is, however, some disagreement between the different data in the energy interval $E_p = 40$–50 MeV. The cross section values at $E_p = 40$ MeV of Refs. [13,12] differ by more than a factor of 2. The same holds for the values around 50 MeV of Refs. [12,14]. As no systematic deviation of one of the data sets can be observed, no cross section value was discarded. We therefore fitted the excitation function curve above 23 MeV. Assigning the same weight to each data point, the overall shape of the excitation function curve from 23 to 146 MeV could be best fitted by a power law plus a constant. The fit is very close to the curve in Fig. 3 of Ref. [3] for this reaction. The obtained cross sections values are given in Table I.

For proton energies below 50 MeV, that reaction should proceed principally from a sequential process with the excitation of intermediate states of ^{16}O, decaying subsequently to $\alpha + ^{12}$C$^*_{4.439}$. Reactions with other particles than the α particle in the outgoing channel, such as ^{3}He$+n$ or ^{3}H$+p$ have thresholds ≈ 20 MeV higher, around $E_p = 35$ MeV, and should be negligible for the production of ^{12}C$^*_{4.439}$ in solar flares. The sequential character can be deduced from a study of the ^{16}O$(p,p\alpha)^{12}$C reaction at a proton energy of 46.8 MeV, where no evidence for quasielastic p-α scattering was found [16]. Still other reaction paths, such as ^{16}O$(p,\alpha)^{13}$N$^* \rightarrow p + ^{12}$C$^*_{4.439}$ were also found negligible. At lower energies these reaction mechanisms should be still weaker. We adopted in the following exclusively the sequential process ^{16}O$(p,p')^{16}$O$^* \rightarrow \alpha + ^{12}C^*_{4.439}$.

Parameters entering into the line shape determination are therefore the relative contribution of the different excited states in ^{16}O and for each excited state the differential cross section with respect to the recoiling ^{16}O* scattering angle, the ^{12}C*-^{16}O angular correlation and the γ-^{12}C angular correlation. Given the scarcity of experimental data and the number of excited states involved, it is highly impracticable if not impossible to undergo a full and correct calculation for numerous proton energies from threshold to 100 MeV. One can, however, reasonably assume that the average angular

TABLE I. Cross section σ and mean excitation energies for the spallation reaction ^{16}O$(p,p\alpha)^{12}$C$^*_{4.439}$ and parameter p of the inelastic scattering angular distributions ^{16}O(p,p'). ($E_p = 16$–20 MeV): Mean excitation energies $\mathcal{E}_x$ in ^{16}O from the adjustment of the 4.438 MeV γ-ray lines of the Orsay experiment [8]. Isotropic inelastic scattering angular distributions were used ($p=0$). ($E_p = 22.5$–100 MeV): Mean excitation energies $\mathcal{E}_x$ in ^{16}O and fit parameter p of the inelastic scattering angular distributions ^{16}O(p,p') obtained by OM calculations. For $E_p < 16$ MeV, the values of 16 MeV were used.

E_p (MeV)	σ (mb)	$\mathcal{E}_x$ (MeV)	p (deg^{-1})
14	3	12.75	0.0
15	16	12.75	0.0
16	40	12.75	0.0
17	64	13.25	0.0
18	85	14.0	0.0
20	140	14.75	0.0
22.5	156	14.7	0.001
25	137	15.5	0.008
30	95	17.1	0.009
40	55	18.0	0.027
45	44	18.3	0.030
66	24	18.5	0.057
100	14	18.5	0.078

distribution of the α-^{12}C* decay in the recoiling ^{16}O* system and the angular distribution of the γ-ray emission in the ^{12}C* system are isotropic, because of the contribution of many ^{16}O levels with different spin and parity (see the discussion in Ref. [13]).

A. $E_p = 16$–20 MeV

In this energy range, experimental line shapes are available from a recent accelerator experiment at Orsay [8] at six different γ-ray detection angles, ranging from 45° to 145° with respect to the incoming beam direction and at four proton energies. These experimental line shapes were compared with calculated ones obtained with the use of a Monte Carlo type program. In this program reaction parameter inputs were the differential cross section with respect to the proton center-of-mass scattering angle and the mean excitation energy in ^{16}O. As mentioned above, the vector of the α-^{12}C* decay in the ^{16}O* system and the γ-ray emission in the ^{12}C* system were taken isotropically. Slowing down of the carbon in the target with exponentially decaying γ-ray emission probability corresponding to the lifetime of the 4.439 MeV state, as well as the full detector geometry and resolution were taken into account to generate theoretical detector spectra. Stopping powers were taken from the code TRIM [17].

Optical-model calculations of inelastic proton scattering off ^{16}O to states from 12.75 to 17 MeV, with optical potential parameters from the compilation of Perey and Perey [19] were performed to obtain the differential inelastic scattering cross sections $d\sigma/d\Omega_{p_{\text{c.m.}}}$. The calculated cross sections were found to be roughly isotropic in this proton energy
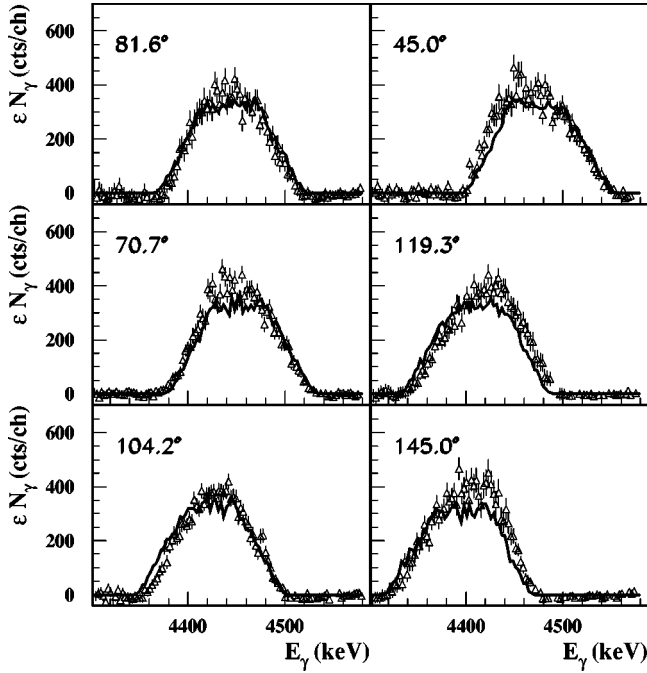
FIG. 1. Experimental spectra from the Orsay experiment [8] of the 4.438 MeV γ-ray line (open triangles) from the proton induced spallation of ^{16}O at $E_p = 20$ MeV and results of a Monte Carlo simulation of the experiment (full line) with a constant differential cross section in the center-of-mass proton diffusion angle and a mean excitation energy of $E_x = 14.75$ MeV. Note that the experimental spectra at the different detector angles have been corrected for the individual relative detector efficiencies. The fact that the simulation with isotropic angular distributions predicts correct relative line intensities (with a common absolute normalization factor) indicates therefore an isotropic angular distribution of the γ rays in the laboratory.

range. Furthermore the calculated line shapes proved to be not very sensitive to the details of the differential cross section, we simply used a constant $d\sigma/d\Omega_{p_{c.m.}}$. The mean excitation energy $\mathcal{E}_x$ in ^{16}O was then the only parameter that has been adjusted to reproduce the experimental γ-ray spectra.

Figure 1 shows the result of a line shape calculation at $E_p = 20$ MeV for the six detection angles of the experiment. Position, line shape, and relative intensities of the experimental lines are fairly well reproduced by the calculation, which gives credit to the validity of the assumption of essentially isotropic angular distributions. We also checked that calculations with a Gaussian distribution of the excitation energy centered at $\mathcal{E}_x$ resulted in practically identical line shapes. Those calculations have been made at the four proton energies where experimental spectra were extracted. The obtained mean excitation energies are presented in Table I.

B. $E_p = 20-100$ MeV

In this proton energy range, some experimental information on line shapes and on inelastic cross sections of excited levels in ^{16}O are available at $E_p = 40$, 45, and 46.8 MeV [13,18,16]. Lang et al. [13] deduced relative contributions to the ^{12}C$^*_{4.439}$ production for ^{16}O states ranging from E_x

$= 12.53$ to 28 MeV from the cross sections at $\Theta_p = 40°$ and $E_p = 45$ MeV of Buenerd et al. [18]. For excitation energies above 28 MeV, virtually no contribution has been observed in the ^{16}O(p,p')^{16}O reaction at $E_p = 45$ MeV [18] and in the ^{16}O($p,p\alpha$)^{12}C$^*_{4.439}$ reaction at $E_p = 46.8$ MeV [16].

We used as the basis of our calculations eight representative states E_i for the ^{16}O levels, with the relative contribution to the ^{12}C$^*_{4.439}$ production P_i:

$$P_i = \frac{\Gamma^i_{\alpha_1}}{\Gamma^i_{tot}} \frac{d\sigma_i}{d\Omega}(40°) \tag{1}$$

given by Lang et al. [13] in their Table I for $E_p = 45$ MeV. Here, $\Gamma^i_{\alpha_1}$ and Γ^i_{tot} mean the partial decay width to the $\alpha + {}^{12}$C$^*_{4.439}$ channel and the total width of the state i, respectively. In detail, we chose the following representative states with excitation energy E_i.

(1) $E_1 = 12.75$ MeV, 2^+, representing the 12.53, 13.02, and 13.26 MeV levels of Ref. [13].

(2) $E_2 = 15.1$ MeV, 2^+, representing the 13.97, 15.27, and 15.50 MeV levels of Ref. [13].

(3) $E_{3-8} = 17$, 19, 21, 23, 25, and 27 MeV, 2^+, representing the respective excitation energy range $E_x = E_i \pm 1$ MeV of Ref. [13].

The choice of exclusively $l = 2$ excitations to 2^+ states has two reasons. First, calculations of inelastic proton scattering to the giant resonance region at $E_x = 21-28$ MeV indicate good agreement of $l = 2$ excitation with the experimental data [18]. Second, the dependence of the cross section on the proton energy proved to be not very sensitive to the multipolarity, and the angular dependence of the cross section for $l = 2$ excitations is somehow intermediate between $l = 1$ and $l = 3$ excitations, simulating fairly well an averaged angular distribution for the three multipolarities. Non-natural parity states and excitations with $l > 3$ are not believed to change the overall trends much.

We also assumed that the total cross section for each state is proportional to the differential cross section at 40°. This was supported by OM calculations for $E_p = 45$ MeV, where the ratio of the inelastic scattering cross section σ_i to the differential cross section $d\sigma_i/d\Omega$ at 40° was found constant to within 20% for the different excited states.

The mean excitation energy for $E_p = 45$ MeV is then simply defined as

$$\mathcal{E}_x = \frac{\sum_i P_i E_i}{\sum_i P_i}. \tag{2}$$

To obtain the mean excitation energy at other proton energies, we made extensive OM calculations with the code ECIS94 [20], using the optical potential parameters of the compilation of Perey and Perey [19]. For each proton energy we calculated the inelastic scattering cross section for the eight representative states of ^{16}O. All calculations were restricted to direct one-step excitation of the respective state in

^{16}O, which should be the main excitation mechanism for the states of interest at these proton energies.

Calculations were done for the following proton energies: $E_p=22.5, 25, 30, 40, 45, 66,$ and 100 MeV. The mean excitation energy as a function of proton energy was calculated in the following way:

$$\mathcal{E}_x(E_p)=\frac{\sum_i P_i E_i \sigma_i(E_p)/\sigma_i(45\ \text{MeV})}{\sum_i P_i \sigma_i(E_p)/\sigma_i(45\ \text{MeV})}. \tag{3}$$

The differential cross sections have been obtained in the same way by averaging over the eight representative states. In order to facilitate line shape calculations for a wide range of proton energies, we parametrized the differential cross section by a simple function

$$\frac{d\sigma}{d\Omega_p}=Ne^{-p\Theta}, \tag{4}$$

where Θ is the proton diffusion angle in the center-of-mass system. It was checked that this simple function produced essentially the same line shapes as the differential cross sections from the OM calculations. The values of $\mathcal{E}_x$ and p are presented in Table I.

III. THE INELASTIC SCATTERING REACTION ^{12}C$(p,p\gamma)$

The cross section excitation function $\sigma(E_p)$ was taken from the measurements of Dyer *et al.* [11] from threshold to 23 MeV, above that from the data of Lang *et al.* [13] and Lesko *et al.* [12] up to 85 MeV, then from the curve of Ramaty, Kozlovsky, and Lingenfelter [3] up to 100 MeV. Cross section values are reported in Table II.

Production of 4.438 MeV γ-ray emission by inelastic scattering off ^{12}C originates mainly from direct excitation of the 2^+, 4.439 MeV level. All higher-lying levels of ^{12}C are particle-unbound and have small to very small γ-branching ratios to the 4.439 MeV state [21], making γ-ray cascade contributions negligible. The γ-ray line shape and the γ-ray angular distribution are in this case completely determined by the double differential inelastic cross section $d^2\sigma/d\Omega_p d\Omega_\gamma$. It can be expressed as a product of the differential cross section $d\sigma/d\Omega_p$ and the angular correlation function W (see, for example, Satchler [22]):

$$\frac{d^2\sigma}{d\Omega_p d\Omega_\gamma}=\frac{d\sigma}{d\Omega_p}\ \frac{1}{4\pi}\ W(\vec{k},\vec{k}',\vec{k}_\gamma), \tag{5}$$

where $\vec{k}$ and $\vec{k}'$ are the wave vectors of the incoming and outgoing proton, respectively, and $\vec{k}_\gamma$ is the vector of the emitted γ ray.

Although a wealth of differential cross sections are available for this reaction, proton-γ correlation measurements exist only for few proton energies. The angular correlation function must therefore be extracted either from experimen-

TABLE II. Cross section σ and population amplitudes for the inelastic scattering reaction ^{12}C$(p,p)^{12}$C$^*_{4.439}$. ($E_p=8.6-19.75$ MeV): Result of the adjustment of the population amplitudes a_m and the phase shift $\Delta\Phi$ to measured line shapes from the Orsay experiment [8] and γ-ray angular distributions from the Orsay experiment and from the Washington experiment [11]. ($E_p=25-100$ MeV): Result of the adjustment of the population amplitudes a_m and the phase shift $\Delta\Phi$ to line shapes and γ-ray angular distributions resulting from OM calculations. Population amplitudes below 8.6 MeV are an average of the extracted values from 8.6–10.6 MeV. The amplitudes are normalized such that $\Sigma_m a_m^2=1$ and $a_{-m}=a_m$.

E_p (MeV)	σ (mb)	a_0	a_1	a_2	$\Delta\Phi$ (deg)
5	51	0.64	0.27	0.47	30
6	55	0.64	0.27	0.47	30
7	108	0.64	0.27	0.47	30
8	240	0.64	0.27	0.47	30
8.6	270	0.57	0.28	0.51	35
9.0	290	0.66	0.26	0.46	30
9.6	275	0.71	0.35	0.35	30
10.0	265	0.70	0.28	0.42	30
10.6	296	0.59	0.21	0.53	20
11.0	317	0.55	0.33	0.49	35
11.4	298	0.56	0.34	0.45	30
12.0	270	0.55	0.22	0.55	25
12.6	277	0.42	0.08	0.63	25
13.0	282	0.40	0.12	0.64	25
13.6	281	0.42	0.13	0.63	25
14.0	281	0.42	0.13	0.63	25
14.4	255	0.42	0.13	0.63	25
15.2	217	0.42	0.13	0.63	25
16.25	188	0.33	0.03	0.66	20
17.25	166	0.27	0.03	0.68	20
18.25	153	0.27	0.16	0.66	15
19.75	130	0.29	0.20	0.64	15
25	99	0.25	0.025	0.68	112.5
35	69	0.37	0.0	0.66	100
49.5	23	0.43	0.0	0.64	100
75	14	0.51	0.0	0.61	95
100	11	0.58	0.0	0.58	90

tal data, for example by fitting of γ-ray angular distributions and line shapes or be obtained from OM calculations. The excitation function for the 4.438 MeV γ-production cross section exhibits pronounced fluctuations from threshold up to ≈ 15 MeV (see Ref. [8] or [11]). This indicates strong contributions of compound nucleus resonances ^{12}C$+p\rightarrow^{13}$N* $\rightarrow p+^{12}$C$^*_{4.439}$ to the inelastic scattering.

Because OM calculations are only suited for the direct reaction mechanism, their use in this energy range was discarded. We used the measured line shapes and γ-ray angular distributions of the Orsay experiment [8] and published data for $d\sigma/d\Omega_p$ for $E_p=8.6-20$ MeV to adjust the parameters of the correlation function. Some available γ-ray angular distributions of the Washington experiment [11] were also used for comparison. The parameter adjustment was achieved by

reproducing as closely as possible the experimental data in extensive calculations with the Monte Carlo type program simulating the reaction and the detection setup of the Orsay experiment.

At higher proton energies, Meigooni *et al.* [9] provide a phenomenological optical potential for neutron and proton scattering off ^{12}C, which reproduces fairly well elastic and inelastic scattering angular distributions. The OM calculations were used to obtain the necessary input parameters for the calculation of the double differential cross section $d^2\sigma/d\Omega_p d\Omega_\gamma$.

A. $E_p = 8.6 - 20$ MeV

We adopted the formalism used in Refs. [3,7] for the proton-γ angular correlation and the calculation of the γ-ray line shape. In this formalism, the angular correlation function W is expressed in the rest frame of the recoiling excited ^{12}C$^*_{4.439}$ nucleus, whose recoil angle and velocity is kinematically fixed by the incoming and outgoing proton wave vectors $\vec{k}$ and $\vec{k}'$. The correlation function W then reduces to the γ-ray angular distribution $W(\Theta,\Phi)$ in the carbon rest frame. It is proportional to the radiation pattern $dP/d\Omega$, which depends on the magnetic substate population amplitudes $a_m(\vec{k},\vec{k}')$ of the 4.439 MeV, 2^+ state of ^{12}C (see, e.g., Jackson [23]):

$$\frac{dP}{d\Omega} = \frac{c}{8\pi k^2}\left|\sum_{m=-2}^{2} i a_m(\vec{k},\vec{k}')\vec{X}_{2m}(\Theta,\Phi)\right|^2, \quad (6)$$

where the $\vec{X}_{2m}$ are the vector spherical harmonics for quadrupole radiation, and Θ, Φ the polar and azimuthal angles of the γ-ray emission in the rest frame of the excited carbon. The aim was to find a set of population amplitudes $a_m(\vec{k},\vec{k}')$ for each proton energy of the Orsay experiment, which gives simultaneously a good reproduction of the experimental line shapes and the laboratory γ-ray angular distribution.

Kozlovsky, Ramaty, and Lingenfelter [7] obtained reasonable fits of the six experimental line shapes at $E_p = 23$ MeV from Ref. [24] by adjusting only two independent real amplitudes, which furthermore were independent of the proton diffusion angle. We started our search with the same simple basis and adjusted the two independent relative amplitudes a_2/a_0 and a_1/a_0 (with a_m real, $a_{-m} = a_m$ and $\Sigma a_m^2 = 1$), independent of the carbon recoil angle. However, these two parameters were not sufficient and it proved to be necessary for a simultaneous reproduction of the line shapes and the γ-ray angular distribution to introduce a third independent parameter. We found that a phase shift $\Delta\Phi$ for the azimuthal angle improved considerably the fits and gave a satisfactory reproduction of the Orsay data at most proton energies.

Practically, for the search of the population amplitudes, we used as in the case of the spallation reaction a Monte-Carlo type program simulating the nuclear reaction and the detection system of the Orsay experiment. For each proton center-of-mass diffusion angle, the ^{12}C$^*_{4.439}$ recoil direction and energy were calculated in the laboratory system. For the

γ-ray emission, we chose a coordinate system with origin in the recoiling carbon nucleus, the z axis perpendicular to the scattering plane and the x axis in the direction of the carbon velocity vector. Θ defines the angle between the γ-ray vector and the z axis, while Φ is defined as the angle between the x axis and the projection of the γ-ray vector on the scattering plane, counted counterclockwise from the x axis. Subsequently, the γ-ray vector was calculated in the laboratory system and the energy of the γ ray was stored when it was in the solid angle of one of the detectors. Again, slowing down of the recoiling excited ^{12}C in the target and decay of the 4.439 MeV state with half-life $\tau_{1/2} = 42$ fs were taken into account.

Because of the presence of multiple compound nucleus resonances in this energy range, calculations were done in narrow proton energy steps between 8.6 and 20 MeV. For each energy, population amplitudes were adjusted to reproduce the γ-ray line shapes of the six detectors and special care was taken to obtain a simultaneously good reproduction of the laboratory γ-ray angular distribution. For $d\sigma/d\Omega_p$, experimental cross sections of Peelle [25] for $E_p = 14$–19.4 MeV and of Barnard, Swint, and Clegg [26] for $E_p = 8.6$–11.6 MeV were used. For $E_p = 11.6$–14 MeV we interpolated between the differential cross sections of Ref. [26] at 11.6 MeV and Ref. [25] at 14 MeV. The results of the adjustments are presented in Table II and an example of calculated line shapes and laboratory γ-ray angular distribution is shown in Fig. 2 together with data of the Orsay [8] and Washington [11] experiments.

B. $E_p = 20 - 100$ MeV

Experimental data in this energy domain are relatively scarce, and no systematic measurements of differential cross sections $d\sigma/d\Omega_p$ and $d\sigma/d\Omega_\gamma$ or line shapes are available. However, Meigooni *et al.* [9] performed a systematic study of nucleon elastic and inelastic scattering off ^{12}C and found an energy dependent optical potential parameter set, which provides good fits to measured differential cross sections in a wide angular range and for energies above the pronounced compound nucleus contributions (≈ 15 MeV) up to approximately 100 MeV. We therefore based our calculations entirely on OM calculations with their parameter set.

These calculations were done with the program ECIS94 [20] to obtain the scattering amplitudes $T_{M'_A, M'_a, M_A, M_a}(\vec{k},\vec{k}')$ necessary for the construction of the correlation function W [Eq. (5)]. M_A (M'_A) and M_a (M'_a) are the z components of the ^{12}C and the proton spin in the incoming (outgoing) channel, respectively. Choosing the z axis along the incoming proton direction $\vec{k}$, the amplitudes, correlation function, and consequently the proton and γ-emission angle are directly given in a space-fixed system with respect to the beam direction of the experiment. The correlation function W for emission of the γ ray in the direction $\vec{k}_\gamma$ is given by

$$W(\vec{k},\vec{k}',\vec{k}_\gamma) = \sum_{kq} t_{kq}(\vec{k},\vec{k}')R^*_{kq}, \quad (7)$$

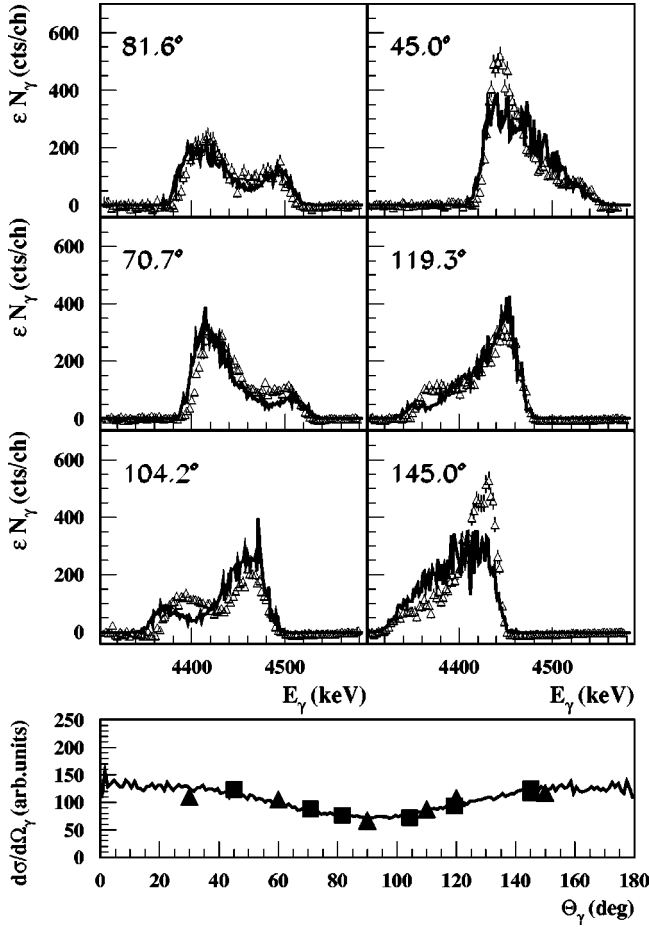where t_{kq} denotes the polarization tensor. It is constructed

FIG. 2. Upper part: Line shapes for the 4.438 MeV γ ray at six different detection angles from proton inelastic scattering off ^{12}C at $E_p = 19.75$ MeV. Triangles: count spectra of the Orsay experiment [8]; full line: calculated line shapes with the population amplitude method. Lower part: Laboratory γ-ray angular distribution from that reaction. Full squares: data from the Orsay experiment; full triangles: experimental data of the Washington experiment [11] at $E_p = 20$ MeV, normalized to the Orsay data; full line: calculated distribution with the population amplitude method.

from the scattering amplitudes T and contains all information on the state of polarization of the excited carbon after scattering (see Satchler [22], Sec. 10.3.3). R_{kq} are the radiation tensors

$$R_{kq} = R_k(\gamma) \sqrt{\frac{4\pi}{2k+1}} Y_k^q(\Theta_\gamma, \Phi_\gamma), \qquad (8)$$

where $R_k(\gamma)$ are the gamma-radiation parameters and Y_k^q the spherical harmonics.

Introducing this correlation function in a program similar to the Monte Carlo type program described above, we calculated theoretical line shapes and γ-ray angular distributions in the laboratory, using the differential cross sections $d\sigma/d\Omega_p$ obtained from OM calculations. Comparison with the Orsay data for $E_p = 16$–20 MeV gave fairly good reproductions of the line shapes and γ-ray angular distributions. An example is shown in Fig. 3 for $E_p = 19.75$ MeV. Given
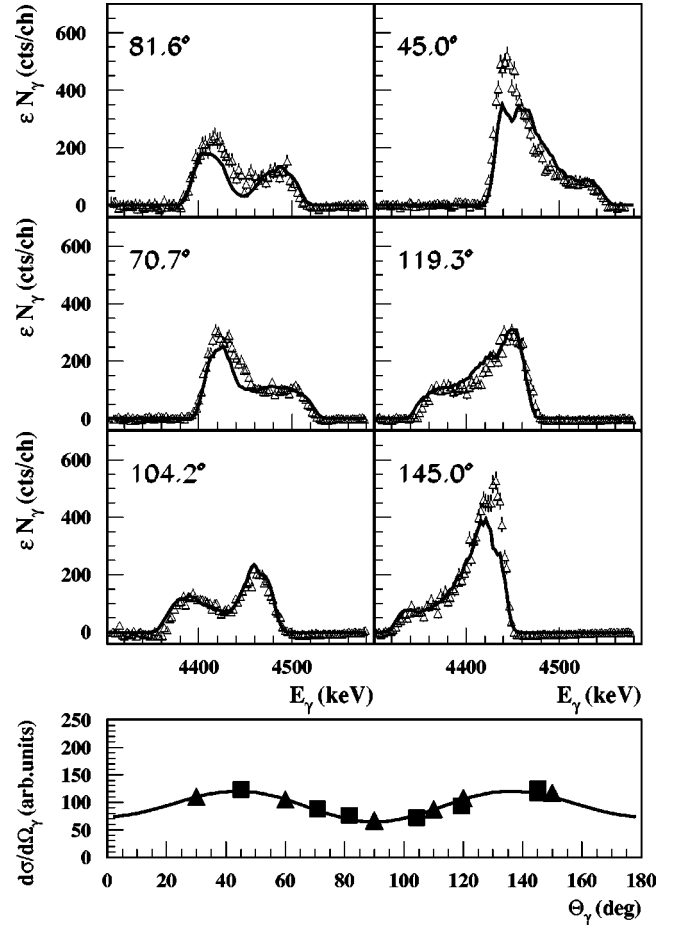
FIG. 3. Same as Fig. 2, except full lines: line shapes and γ-ray angular distribution resulting from OM calculations.

the tendency that the differential cross sections are better reproduced with increasing proton energy (see Ref. [9]), the calculated line shapes and γ-ray angular distributions should be fairly realistic above 20 MeV.

Those calculations are, however, quite complex, involving for each proton energy the input of five complex scattering amplitudes depending furthermore on the proton center-of-mass scattering angle. In order to facilitate line shape calculations for proton spectra covering a wide energy range as in solar flares or cosmic rays, the line shapes and γ-ray angular distributions from the OM calculations for $E_p > 20$ MeV were adjusted with the population amplitude method described in Sec. III A. The population amplitudes and phase shifts from these adjustments are reported in Table II.

IV. α-PARTICLE INDUCED REACTIONS

As in the case of proton induced reactions, the main source of 4.438 MeV γ rays by accelerated α particles is inelastic scattering off ^{12}C and spallation of ^{16}O. The cross section excitation functions being quite similar for both projectiles, reactions with α particles should generally not contribute significantly to the γ-ray line due to their low abundance, e.g., an observed α/p ratio of 0.035 and 0.0076 in the energetic particle spectrum of two solar flares [27].

However, α/p ratios in excess of 0.1 for the accelerated particle spectrum were shown to be necessary for an acceptable fit of the γ-ray spectrum of the 1981 April 27 flare [4]. α-particle reactions are furthermore favored in the case of a very soft particle spectrum, because the thresholds for inelastic scattering off ^{12}C and spallation of ^{16}O are lower for α particles (≈ 2 and 5 MeV per nucleon, respectively) than for protons (≈ 6 and 14 MeV, respectively). In such cases, an important fraction of the γ-ray production may be due to reactions with α particles. Therefore, a treatment of α-particle reactions similar to the above described studies on proton reactions seems worthwhile.

Unfortunately, experimental line shapes are practically absent for α-particle inelastic scattering off ^{12}C and do not exist for α-particle induced spallation of ^{16}O. Concerning spallation of ^{16}O, this may not be very problematic because of the excitation of many intermediate levels in ^{16}O resulting in essentially isotropic γ-ray angular distributions as for ^{16}O$(p,p\alpha\gamma)$. Optical model calculations should then provide as for proton induced spallation a reasonable estimation of the mean excitation energy in ^{16}O and approximate differential inelastic cross sections. On the contrary, inelastic α-particle scattering off ^{12}C is certainly dominated at energies below $E_\alpha \approx 30$ MeV by compound nucleus resonances due to the pronounced α-particle structure of ^{12}C and ^{16}O, making OM calculations very hazardous in this energy range.

A. The spallation reaction ^{16}O$(\alpha,x\gamma)^{12}$C

We made the same assumptions as for the case of proton induced spallation of ^{16}O. Only the sequential process of excitation of intermediate levels in ^{16}O with subsequent decay in α and ^{12}C$^*_{4.439}$ was considered. The angular distributions of the excited carbon in the system of the excited oxygen and of the γ ray in the system of the excited carbon were both considered isotropic.

Because of the absence of experimental line shapes, the estimation of the mean excitation energy in ^{16}O was entirely based on OM calculations and the α-particle energy spectrum of Lang et al. [13], obtained at $E_\alpha = 60$ MeV and at a scattering angle of 12.5°. Contrary to proton scattering, the ratio of the total inelastic scattering cross section to the differential cross section at 12.5° shows a systematic dependance on the excitation energy in the considered range $E_x = 12.53–28$ MeV. Therefore, the relative contributions $d\sigma_i/d\Omega(12.5°)$ extracted from the spectrum of Ref. [13], were multiplied by this ratio to obtain the relative inelastic scattering cross sections σ_i at $E_\alpha = 60$ MeV. Finally, for the partial γ-production probability P_i at 60 MeV, the inelastic scattering cross sections were multiplied with the branching ratios $\Gamma^i_{\alpha_1}/\Gamma^i_{\text{tot}}$, proposed by Ref. [13].

Extensive OM calculations were done for α-particle energies $E_\alpha = 18–400$ MeV and the same eight representative excited ^{16}O states as in Sec. II B to estimate their relative contribution P_i at other projectile energies. As in the proton case, we restricted the calculations to direct one-step $l = 2$ excitations. The energy-dependent phenomenological optical potential of Michel et al. [28], which gives good to very

TABLE III. Estimated cross section σ of the spallation reaction, fit parameters p and C_2/C_1 of the inelastic scattering angular distributions ^{16}O(α,α') and mean excitation energy $\mathcal{E}_x$ of ^{16}O deduced from OM calculations for the spallation reaction ^{16}O$(\alpha,2\alpha)^{12}$C$^*_{4.439}$.

E_α (MeV)	σ (mb)	p (deg^{-1})	C_2/C_1	$\mathcal{E}_x$ (MeV)
18	0.22	0.020	0.12	12.8
20	19	0.017	0.01	12.8
22	44	0.012	-0.08	13.0
24	102	0.009	0.06	13.8
26	125	0.008	0.27	14.2
28	124	0.005	0.51	14.5
30	123	0.003	0.61	14.8
35	120	0.001	1.91	15.7
40	117	0.010	0.94	16.3
50	111	0.019	0.99	16.6
60	139	0.015	0.42	17.1
100	223	0.074	0.0	18.4
150	172	0.125	0.0	18.8
250	100	0.31	0.0	19.0
400	53	0.51	0.0	19.0

good fits of elastic differential cross sections from about 20 to 146 MeV, were used in the entire energy range. From the same calculations, averaged differential cross sections were constructed and their angular distributions fitted by a parametrization as in Sec. II B, but with the addition of a term $\cos^4(\Theta)$ to take account of the backward enhancement of the differential cross sections

$$\frac{d\sigma}{d\Omega} = C_1 e^{-p\Theta} + C_2 \cos^4(\Theta). \qquad (9)$$

For this reaction, the γ-ray production cross section has only been measured at five α-particle energies by Dyer et al. [29] from 22 to 26 MeV and by Zobel et al. [14] at $E_\alpha = 52$ MeV. An estimated cross section curve is given in Ref. [3], however, based on the then only available cross section data of Ref. [14] and limited to α-particle energies below 20 MeV per nucleon. We therefore made a new estimation extending the energy range from threshold to 100 MeV per nucleon. Our best guess, based on the energy dependence of the $(\alpha,4pxn)$ spallation data of Lange et al. [30] and the OM calculations, is a linear interpolation between the cross sections at 26 and 52 MeV. Below 22 and above 52 MeV, we take the energy dependence of the OM calculations. The results of the calculations for the mean excitation energy, the inelastic scattering angular distributions and the γ-ray production cross sections are presented in Table III.

B. The inelastic scattering reaction ^{12}C$(\alpha,\alpha\gamma)$

As already mentioned, practically no line shapes are available for this reaction and OM calculations at low α-particle energies are not believed to be very realistic. To get an idea of the magnetic substate population amplitudes anyway, we employed two different methods at energies be-
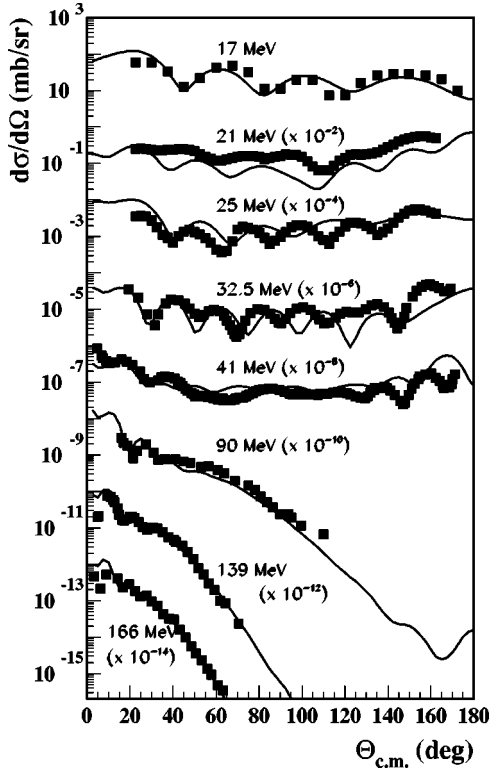
FIG. 4. Experimental differential inelastic cross sections $^{12}C(\alpha,\alpha')^{12}C$ (filled squares, Refs. [31–37]) and results of OM fits (full lines).

TABLE IV. Cross section σ and results of the adjustment of the population amplitudes a_m and the phase shift $\Delta\Phi$ to measured and calculated line shapes and γ-ray angular distributions for inelastic α-particle scattering to the 4.439 MeV, 2^+ state of ^{12}C. The amplitudes are normalized such that $\Sigma_m a_m^2 = 1$ and $a_{-m} = a_m$; $a_{\pm1} = 0$.

E_α (MeV)	σ (mb)	a_0	a_1	a_2	$\Delta\Phi$ (deg)
8	48	0.0	0.0	0.71	-5
9	72	0.0	0.0	0.71	-5
10	231	0.0	0.0	0.71	-5
11	347	0.0	0.0	0.71	-5
12	393	0.0	0.0	0.71	-5
13	361	0.0	0.0	0.71	-10
14	431	0.14	0.0	0.70	-22.5
15	381	0.0	0.0	0.71	-12.5
16	371	0.17	0.0	0.70	-22.5
17	306	0.27	0.0	0.68	-32.5
21	276	0.68	0.0	0.52	-102.5
25	292	0.65	0.0	0.54	-90
32.5	141	0.61	0.0	0.56	-90
41	94	0.37	0.0	0.66	-55
90	45	0.37	0.0	0.66	-70
139	27	0.45	0.0	0.63	-70
166	26	0.40	0.0	0.65	-75
250	18	0.37	0.0	0.66	-80
400	6	0.58	0.0	0.58	-80

low 30 MeV. From $E_\alpha = 8–17$ MeV, we used the systematic measurements of differential cross sections $d\sigma/d\Omega_\alpha$ and laboratory γ-ray angular distributions $d\sigma/d\Omega_\gamma$ of Mitchell, Carter, and Davis [31] and Ophel *et al.* [32]. We then used the Monte Carlo type program described in Sec. III A to find a set of population amplitudes a_m (with $a_m = a_{-m}$, and here throughout $a_{\pm1} = 0$ for $0^+ \to 2^+$ excitations induced by inelastic α-particle scattering on spin-0 targets such as ^{12}C) and phase shifts $\Delta\Phi$ which reproduces the measured γ-ray angular distributions.

Morgan and Hobbie [33] measured in small energy steps between $E_\alpha = 19–30$ MeV inelastic differential cross sections. However, no γ-ray angular distributions or line shape measurements are available in that energy range. Therefore, we used OM calculations despite the fact that compound nucleus resonances are probably important below $E_\alpha = 30$ MeV. In order to reduce the effect of individual compound nucleus resonances, we averaged several differential cross sections of Ref. [33] centered around the α-particle energies of 21 and 25 MeV. Between 30 and 200 MeV, we used the inelastic scattering data of Burdzik and Heymann at 32.5 MeV [34], of Baron, Leonard, and Stewart [35] at 41 MeV, of D'Agostino *et al.* at 90 MeV [36], of Smith *et al.* at 139 MeV [37], and of Tatischeff and Brissaud at 166 MeV [38]. With these differential cross sections OM fits were then done, again with the optical potential of Michel *et al.* [28]. Results of the OM fits in the energy range $E_\alpha = 17–166$ MeV are shown in Fig. 4. Above 200 MeV, no inelastic differential cross sections are published. We contin-

ued to use the optical potential shape of Michel *et al.* for the inelastic scattering calculations, extrapolating up to 400 MeV the optical potential found at 166 MeV by following the energy dependence of the potential parameters given by Michel *et al.* for α-particle scattering off ^{16}O.

Again, as for proton inelastic scattering off ^{12}C, the line shapes and γ-ray angular distributions predicted by the OM calculations were used to deduce population amplitudes and phase shifts for a consistent parametrization of the γ-ray emission in proton and α-particle inelastic scattering off ^{12}C in the energy range of interest for solar flares and low-energy cosmic rays. The cross section excitation function is taken from Dyer *et al.* [29] for $E_\alpha = 8–26$ MeV, from the data of Refs. [34–38] at 32.5, 41, 90, 139, and 166 MeV, respectively, and from our OM calculations at 250 and 400 MeV. Results for the population amplitudes, phase shifts and total cross sections are presented in Table IV.

V. PREDICTED LINE SHAPES IN SOLAR FLARES AND DISCUSSION

With the above deduced reaction parameters, the line shape of the 4.438 MeV γ ray emitted from the first excited state of ^{12}C for proton and α-particle interactions with ^{12}C and ^{16}O can be calculated for energies from threshold up to 100 MeV per nucleon. To illustrate the line shapes that can be expected from solar flares, we use a simple model of γ-ray production by energetic particle interactions in a thick target. For the accelerated particle energy distribution $N(E)$,
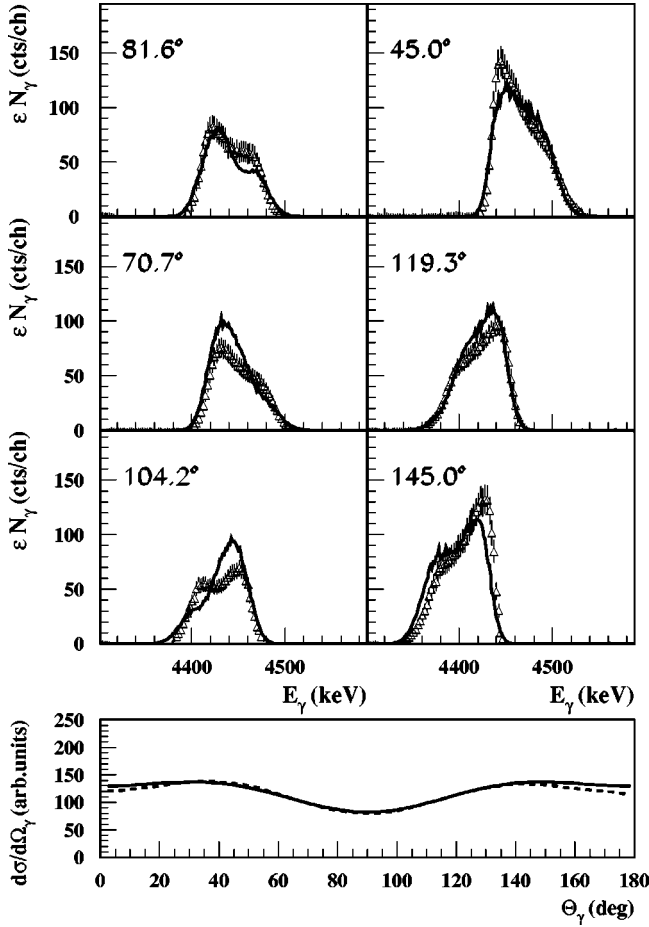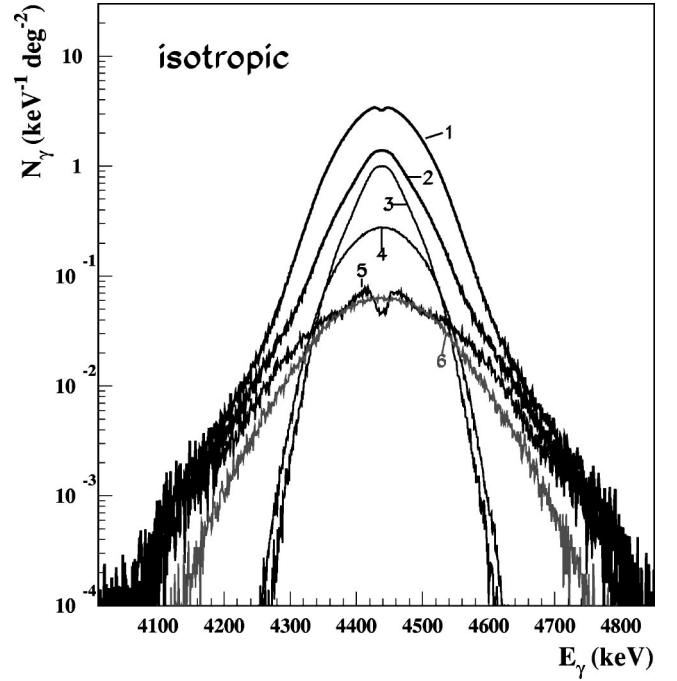
FIG. 6. Emitted line profiles of the 4.438 MeV γ ray for flares with isotropic energetic particle distribution. Curves 1 and 2 are the profiles resulting from energetic proton and α-particle interactions with ^{12}C and ^{16}O with spectral parameters $s=2.4$; $E_0=300$ MeV and $s=3.3$; $E_0=30$ MeV, respectively. Curves 3–6 show the different contributions for the soft particle spectrum. They are in detail (3) ^{12}C$(p,p\gamma)$, (4) ^{16}O$(p,p\alpha\gamma)$, (5) ^{12}C$(\alpha,\alpha\gamma)$, (6) ^{16}O$(\alpha,2\alpha\gamma)$.

FIG. 5. Upper part: Line shapes for the 4.438 MeV γ ray from proton inelastic scattering off ^{12}C summed for $E_p=8.6$–20 MeV. The summation has been done with a weight factor for each proton energy following the thick-target interaction probability of a incident proton spectrum as given in Eq. (10). Parameters of the spectrum were $s=3.3$; $E_0=30$. The summed experimental spectra from the Orsay experiment [8] are presented by open triangles while the summed spectra constructed with the population amplitudes method are shown by the full line. Lower part: Summed laboratory γ-ray angular distributions. The summed experimental distributions are constructed from Legendre-polynom fits of the Orsay data and are shown by the full line, while the dashed line shows the angular distribution resulting from the population amplitudes method.

we choose a spectrum as it results from diffuse shock acceleration [27]:

$$N(E) \propto \frac{1}{v} p^{-s} \exp(-E/E_0), \qquad (10)$$

where v and p are the particle velocity and the momentum per nucleon, respectively; s and E_0 are the spectral index and cutoff energy, specific to a given acceleration site. The energies labeled E, E_0, E_{max}, E' in Eqs. (10),(11) and in the following are expressed in energy per nucleon. The total number of 4.438 MeV γ rays N_γ produced by interactions of projectiles of type i (p or α) with target nuclei of type j is then given by

$$N_\gamma=[A_j]n\times\int_0^{E_{max}}\frac{\sigma_{ij}(E)dE}{dE/dx_i(E)}\times\int_E^{E_{max}}N_i(E')dE', \qquad (11)$$

where $[A_j]$ is the abundance of isotope j with respect to hydrogen and n the density of hydrogen atoms at the interaction site; $\sigma_{ij}(E)$ is the γ-ray production cross section and $dE/dx_i(E)$ is the stopping power of particle i. We made the simplifying assumption that the energy loss is only due to the electronic stopping power in a neutral gas, consisting of hydrogen and helium with [He]/[H]=0.1. The Bethe formula was used for the energy loss calculation.

We adopted two sets of s and E_0: $s=3.3$; $E_0=30$ MeV and $s=2.4$; $E_0\geqslant300$ MeV corresponding to the fit of interplanetary proton observations of two distinct solar flares [27]. We set $[O]=0.068\%$, $[C]=0.042\%$ as in Ref. [27], $E_{max}=2\times E_0$, and an α/p ratio of 0.1.

In both cases, proton interactions dominate; they account for 82 and 84 % of the γ-ray production with the softer and harder spectrum, respectively. With the softer spectrum, the γ-ray production is dominated by proton inelastic scattering off ^{12}C (57%), of which in particular 85% of the γ rays are produced by interactions at proton energies below 20 MeV. In order to get an overall impression of the quality of reproduction of the γ-ray lines from the important low energy proton inelastic scattering reactions, energy integrated data from the Orsay experiment were produced and compared
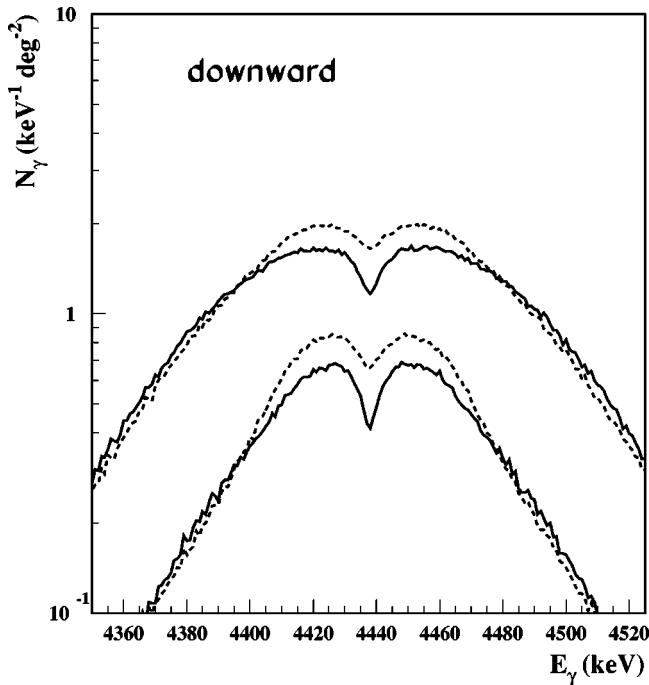
FIG. 7. Emitted line profiles of the 4.438 MeV γ ray for downward flares at the solar limb, i.e., for a detection angle of 90° with respect to the energetic particle direction. The upper two curves are for an energetic particle spectrum with $s=2.4$; $E_0=300$ MeV, the lower two curves are for $s=3.3$; $E_0=30$ MeV. Full lines are the profiles calculated with population amplitudes from this work; for comparison, the dashed lines are calculated with population amplitudes from the parametrization proposed by Murphy, Kozlovsky, and Ramaty [5].
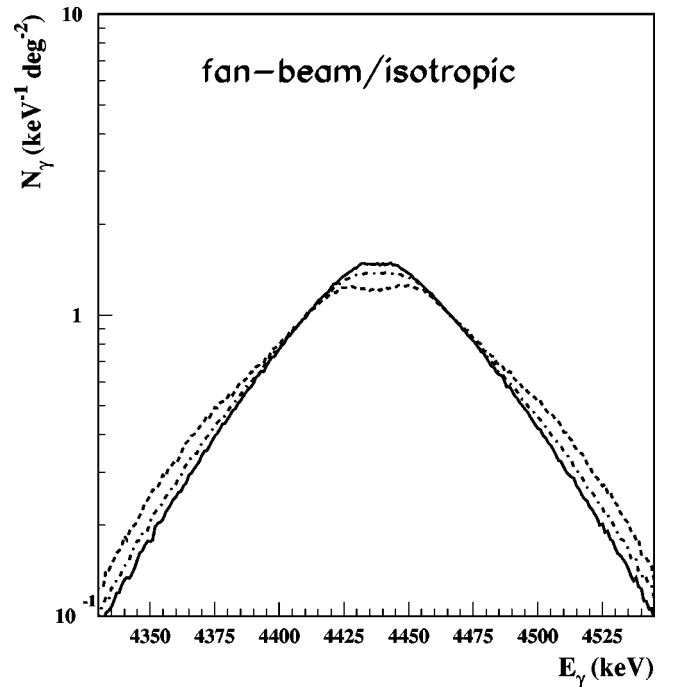
FIG. 8. Emitted line profiles of the 4.438 MeV γ ray for two fan-beam flares and an isotropic flare with energetic particle spectrum parameters $s=3.3$; $E_0=30$ MeV. The full line is for a fan-beam flare occuring at the solar disk, with an angle Θ_{flare} between the line-of-sight and the flare symmetry axis of 135° and an angular distribution proportional to $\sin^6(\Theta_p)$, Θ_p being the angle between the particle direction and the flare symmetry axis. The dashed line shows the profile for the same flare occuring at the solar limb ($\Theta_{\text{flare}}=90°$), and the dashed-dotted line the profile for an isotropic interaction probability.

with the calculations. Line shapes and γ-ray angular distributions for energy integrated experimental and calculated data between 8 and 20 MeV for proton inelastic scattering off ^{12}C, are represented in Fig. 5.

For the relatively hard spectrum with $s=2.4$ and setting $E_0 = 300$ MeV, proton induced spallation of ^{16}O is the strongest channel, accounting for 46% of the 4.438 MeV γ rays. Here, proton interactions at energies below 20 MeV are responsible for 24% of the total γ-ray production, α and proton interactions at energies below 100 MeV account for 83% of the produced γ rays. These values, however, have to be regarded as lower limits only, because secondary protons of low and intermediate energy produced by high energy proton and α particles and escape of accelerated particles into interplanetary space are not taken into account.

For the prediction of γ-ray line profiles from solar flares we calculate the interaction probability as in Eq. (11). No absorption or Compton scattering of the produced 4.438 MeV γ ray in the solar atmosphere is taken into account. Three different energetic particle angular distributions have been investigated, similar to the distributions investigated by Murphy, Kozlovsky, and Ramaty [5]: an isotropic angular distribution, a fan-beam flare, and a downward flare. The narrow component of the 4.438 MeV γ ray is shown in Figs. 6, 7, and 8 for the different energetic particle angular distributions and energy spectra, all with an α/p ratio of 0.1. All

curves are arbitrarily normalized to a total kinetic energy in proton and α particles with $E>1$ MeV of 10^8 erg.

The narrow component is clearly dominated by the $p+^{12}$C reaction for the soft particle spectrum. Comparing curves 1 and 2 of Fig. 6, which shows the predicted line shapes for isotropic incident particle spectra, it seems possible to estimate the spectral hardness by the width of the line and the characteristic drop around 4.438 MeV only visible for the hard spectrum. This drop, also seen in curve 5 of Fig. 6 is not predicted by other parametrizations, as for example in Ref. [5].

Figure 7 shows the line profiles resulting from a downward directed energetic particle distribution at the solar limb. The parametrization of Ref. [5] for the population amplitudes reproduces qualitatively the characteristic line shape with two intensity maxima above and below the minimum at 4.438 MeV, but it underestimates slightly the maximum-to-minimum ratio and overestimates the intensity (by $\approx 10\%$) emitted at 90°. Line shapes produced by fan-beam distributions and an isotropic distribution as in Fig. 8 will be difficult to distinguish, showing only small differences in the overall line profile.

In summary, with the extracted nuclear reaction parameters in this work, line shape calculations for proton and α-particle induced reactions on ^{12}C and ^{16}O can be done for

all possible energetic particle angular distributions and for particle energies from threshold to about 100 MeV per nucleon, which is the important energy domain for solar flares and low-energy cosmic rays. These parameters can also be straightforwardly used for the inverse reactions, energetic ^{12}C and ^{16}O bombarding proton and α particles.

It is the first parametrization for line shape calculations, which is largely based on experimental data and optical model calculations. Especially, the calculation of γ-ray line shapes from proton induced reactions is certainly very close to reality, as illustrated by the good reproductions of experimental line shapes in Figs. 1 and 5; at higher energies, the optical potential of Ref. [9] is believed to provide line shape reproductions of the same quality. Only line shapes from α-particle induced inelastic scattering below ≈ 10 MeV per nucleon have to be regarded with some caution because of the only moderately successfull OM fits of differential inelastic cross sections. Here, new experimental data for γ-ray line shapes and angular distributions could greatly improve

the parametrization. For α-particle induced spallation of ^{16}O above $E_\alpha = 26$ MeV, γ-ray production cross sections are needed.

This study confirms qualitatively older parametrizations for proton induced reactions constructed with much less experimental data input [3,5], but some of its predictions of line-profile details are slightly different. It shows that extreme particle angular distributions, such as isotropic or unidirectional ones, can be nicely characterized, with even some hope to get an idea of the spectral hardness of the accelerated particle spectrum. High resolution detectors, such as the Ge detectors on the HESSI spacecraft [10] and on the INTEGRAL observatory [39], could be able to resolve the fine structures in the line profiles which carry this information. Together with other γ-ray lines, one may then be able to extract most flare parameters, such as the spectrum, composition, and the angular distribution of the accelerated particles, as well as the isotopic composition of the ambient medium.

[1] W.T. Vestrand, G.H. Share, R.J. Murphy, D.J. Forest, E. Rieger, E.L. Chupp, and G. Kanbach, Astrophys. J., Suppl. Ser. **120**, 409 (1999).

[2] M. Cassé, R. Lehoucq, and E. Vangioni-Flam, Nature (London) **373**, 318 (1995); E. Parizot and L. Drury, Astron. Astrophys. **349**, 673 (1999).

[3] R. Ramaty, B. Kozlovsky, and R.E. Lingenfelter, Astrophys. J., Suppl. Ser. **40**, 487 (1979).

[4] R.J. Murphy, R. Ramaty, B. Kozlovsky, and D.V. Reames, Astrophys. J. **371**, 793 (1991).

[5] R.J. Murphy, B. Kozlovsky, and R. Ramaty, Astrophys. J. **331**, 1029 (1988).

[6] A.M. Bykov, S.V. Bozhokin, and H. Bloemen, Astron. Astrophys. **307**, L37 (1996).

[7] B. Kozlovsky, R. Ramaty, and R.E. Lingenfelter, Astrophys. J. **484**, 286 (1997).

[8] J. Kiener, M. Berheide, N.L. Achouri, A. Boughrara, A. Coc, A. Lefebvre, F. de Oliveira Santos, and Ch. Vieu, Phys. Rev. C **58**, 2174 (1998).

[9] A.S. Meigooni, R.W. Finlay, J.S. Peter, and J.P. Delaroche, Nucl. Phys. **A445**, 304 (1985).

[10] URL http://www.hessi.ethz.ch/; http://hesperia.gsfc.nasa.gov/hessi/

[11] P. Dyer, D. Bodansky, A.G. Seamster, E.B. Norman, and D.R. Maxson, Phys. Rev. C **23**, 1865 (1981); R. Ramaty (private communication).

[12] K.T. Lesko, E.B. Norman, R.-M. Larimer, S. Kuhn, D.M. Meekhof, S.G. Crane, and H.G. Bussell, Phys. Rev. C **37**, 1808 (1988).

[13] F.L. Lang, C.W. Werntz, C.J. Crannell, J.L. Trombka, and C.C. Chang, Phys. Rev. C **35**, 1214 (1987).

[14] W. Zobel, F.C. Maienschein, J.H. Todd, and G.T. Chapman, Nucl. Sci. Eng. **32**, 392 (1968).

[15] K.J. Foley, G.L. Salmon, and A.B. Clegg, Nucl. Phys. **31**, 43 (1962).

[16] M.B. Epstein, J.R. Quinn, S.N. Bunker, J.W. Verba, and J.R. Richardson, Nucl. Phys. **A169**, 337 (1971).

[17] J.F. Ziegler, computer code TRIM, URL http://www.research.ibm.com/ionbeams/

[18] M. Buenerd, P. Martin, P. de Saintignon, and J.M. Loiseaux, Phys. Rev. C **14**, 1316 (1976).

[19] C.M. Perey and F.G. Perey, At. Data Nucl. Data Tables **17**, 1 (1976).

[20] J. Raynal, notes on ECIS94, Report No. CEA-N-272, 1994 (unpublished).

[21] R.B. Firestone, V.S. Shirley, C.M. Baglin, S.Y. Frank Chu, and J. Zipkin, *Table of Isotopes* (Wiley, New York, 1996).

[22] G.R. Satchler, *Direct Nuclear Reactions* (Clarendon, Oxford, 1983).

[23] J.D. Jackson, *Classical Electrodynamics* (Wiley, New York, 1975).

[24] J.J. Kolata, R. Auble, and A. Galonsky, Phys. Rev. **162**, 957 (1967).

[25] R.W. Peelle, Phys. Rev. **105**, 1311 (1957).

[26] A.C.L. Barnard, J.B. Swint, and T.B. Clegg, Nucl. Phys. **86**, 130 (1966).

[27] R.J. Murphy, C.D. Dermer, and R. Ramaty, Astrophys. J., Suppl. Ser. **63**, 721 (1987).

[28] F. Michel, J. Albinski, P. Belery, Th. Delbar, Gh. Grégoire, B. Tasiaux, and G. Reidemeister, Phys. Rev. C **28**, 1904 (1983).

[29] P. Dyer, D. Bodansky, D.D. Leach, E.B. Norman, and A.G. Seamster, Phys. Rev. C **32**, 1873 (1985).

[30] H.J. Lange, T. Hahn, R. Michel, T. Schiekel, R. Rösel, U. Herpers, H.-J. Hofmann, B. Dittrich-Hannen, M. Suter, W. Wölfli, and P.W. Kubik, Appl. Radiat. Isot. **46**, 93 (1995).

[31] G.E. Mitchell, E.B. Carter, and R.H. Davis, Phys. Rev. **133**, B1434 (1964).

[32] T.R. Ophel, Ph. Martin, S.D. Cloud, and J.M. Morris, Nucl. Phys. **A173**, 609 (1971).

[33] J.F. Morgan and R.K. Hobbie, Phys. Rev. C **1**, 155 (1970).

[34] G.F. Burdzik and G. Heymann, Nucl. Phys. **A185**, 509 (1972).

[35] N. Baron, R.F. Leonard, and W.M. Stewart, Phys. Rev. C **4**, 1159 (1971).

[36] P. d'Agostino, G. Fazio, G. Giardina, O.Yu. Goryunov, M. Sacchi, A.A. Shvedov, I.N. Vishnevsky, and I.Yu. Zaiatz, Nucl. Phys. **A583**, 437 (1995).

[37] S.M. Smith, G. Tibell, A.A. Crowley, D.A. Goldberg, H.G. Pugh, W. Reichart, and N.S. Wall, Nucl. Phys. **A207**, 273 (1973).

[38] B. Tatischeff and I. Brissaud, Nucl. Phys. **A155**, 89 (1970).

[39] C. Winkler, Astron. Astrophys., Suppl. Ser. **120**, 637 (1996); URL   http://astro.estec.esa.nl/SA-general/Projects/Integral/integral.html